

Modeling Brain Energy Metabolism and Function: A Multiparametric Monitoring Approach

Larisa Vatov^a, Ziv Kizner^{a,b,c}, Eytan Ruppin^{d,e}, Sigal Meilin^a,
Tamar Manor^a, Avraham Mayevsky^{a,*}

^a*Faculty of Life Sciences, Bar-Ilan University, Ramat Gan 52900, Israel*

^b*Department of Physics, Bar-Ilan University, Ramat Gan 52900, Israel*

^c*Department of Mathematics and Statistics, Bar-Ilan University, Ramat Gan 52900,
Israel*

^d*Department of Physiology, Tel-Aviv University, Tel-Aviv 69978, Israel*

^e*Department of Computer Science, Tel-Aviv University, Tel-Aviv 69978, Israel*

Received: 21 September 2004 / Accepted: 7 April 2005 / Published online: 28 March 2006
© Society for Mathematical Biology 2006

Abstract Mathematical modeling of brain function is an important tool needed for a better understanding of experimental results and clinical situations. In the present study, we are constructing and testing a mathematical model capable of simulating changes in brain energy metabolism that develop in real time under various pathophysiological conditions. The model incorporates the following parameters: cerebral blood flow, partial oxygen pressure, mitochondrial NADH redox state, and extracellular potassium. Accordingly, all the model variables are only time dependent ('point-model' approach). Numerical runs demonstrate the ability of the model to mimic pathological conditions, such as complete and partial ischemia, cortical spreading depression under normoxic and partial ischemic conditions. They also show that, when properly tuned, a model of this type permits the monitoring of only one or two crucial variables and the computation of the remaining variables in real time during clinical or experimental procedures.

Keywords Mathematical model · Brain energy metabolism · Mitochondrial function · NADH redox state · Cortical spreading depression · Cerebral ischemia

1. Introduction

The knowledge of the processes and changes in the tissue metabolic status is of high importance in biomedical research. Moreover, understanding of the

*Corresponding author.

E-mail addresses: mayevsa@mail.biu.ac.il (Avraham Mayevsky), zinovyk@mail.biu.ac.il (Ziv Kizner), rupin@math.tau.co.il (Eytan Ruppin).

pathophysiological mechanisms underlying tissue deterioration and recovery is of paramount clinical interest. To provide a comprehensive representation of metabolism and the pathophysiological state developed in the tissue in real time, it is necessary to keep track of many metabolic variables simultaneously, of which some are hidden since they cannot be measured in principle or with the instruments available at the present time. This calls for the use of mathematical modeling in predicting tissue damage progression.

Mathematical models are always a simplification of the actual phenomena and therefore, different mathematical models can be suggested for the same phenomenon depending on the objectives of the model and the available measurement data (Gershenfeld, 1999). Mathematical constructs and methods are allied with the present extraordinary computing power. Important in this quest is a hierarchy of models (including both analytical and computational apparatuses), which can capture essential quantitative features of experimental data, and efficiently use these to analyze complex biological systems. Several mathematical models of cellular metabolism have been described in the literature (Hatzimanikatis et al., 1995; Bailey, 1998; Gombert and Nielsen, 1999). Some of these are based on the time invariant characteristics of metabolic networks, others—on microbial kinetics. These models are used both for optimizing biotechnological processes and in the field of functional genomics.

Another kind of mathematical models concerns oxidative metabolism in the cerebral cortex, describing oxygen transport from the capillaries to the tissue during functional activation (Hudetz, 1999). In this approach, the partial pressure of oxygen in cerebral tissue was calculated from the diffusion equation for a general cone-shaped tissue geometry. By this model, the behavior of the oxidative metabolic rate during functional activation was predicted.

In a series of reports, mathematical models were applied to study the processes underlying the pathogenesis of tissue damage (Reggia et al., 1997; Revett et al., 1998; Ruppin et al., 1999). Aiming at the investigation of the lengthwise propagation of the tissue damage and taking into account the spatial heterogeneity of the tissue, the authors of the above-referenced works had to consider both the temporal and spatial variability of several key metabolic variables characterizing the tissue state. In contrast, we confine ourselves to a so-called ‘point model,’ where all the variables representing physiological parameters depend on time only.

The goal of our study is to develop and test a mathematical model that permits the exploration of brain tissue metabolism *in real time*, based on several observable and hidden parameters computed via the model. Such a model has the potential to serve as a tool in simulating the effects of new pathophysiological conditions on the brain responses. A sufficiently detailed model of this kind, when properly tuned, can be used to assess the brain tissue functioning even when not all the parameters are monitored in an actual experiment.

In the next section, we discuss the processes of energy metabolism and the merits of using a mathematical model in monitoring the hidden parameters *in vivo*. The model is presented in Section 3.

2. Energy metabolism and brain function

The principle underlying this work is the consideration of the brain tissue *in vivo* as a whole, focusing on the relationship between oxygen supply and demand, on the one hand, and metabolic energy production and consumption, on the other. All tissues of the human body share the basic mechanisms maintaining the balance between energy demand and supply. A continuous supply of metabolic energy is needed for vital activities of the tissue (Mayevsky and Chance, 1982).

Brain cells are dependent on a continuous supply of oxygen for their normal energy metabolism. The brain consumes about 20% of the total O_2 used by the body at any time. The normal functioning of the brain requires a continuous adjustment between oxygen supply and demand, i.e., the oxygen balance. A decrease in O_2 supply or a large increase in O_2 consumption without an adequate compensation results in a failure of vital brain function. This occurs due to a low reserve of dissolved O_2 in the brain tissue.

It is well established that more than 50% of the energy consumed by the brain is needed for a normal Na^+K^+ -ATPase activity (Erecinska and Silver, 1989). ATP is probably the sole form of energy available for cellular functions and is produced by the oxidative phosphorylation process in the mitochondria. There is a direct coupling between the extracellular levels of various ions (such as K^+ , Ca^{2+} , Na^+ , and H^+) and the metabolic activity of the mitochondria. This phenomenon has a bearing on the oxidation–reduction state of the respiratory chain enzymes and is reflected in the ratio between NAD and NADH. A significant decrease in O_2 supply to the brain will cause a decrease in ATP levels along with a rise in NADH. It is followed by the inhibition of the active transport mechanisms (such as Na^+K^+ -ATPase) and elevation of extracellular K^+ levels, until the normal energy supply is restored. The redox state of the mitochondria is a sensitive indicator of the intracellular metabolic state and can be used to evaluate the cellular energy status (Chance et al., 1973; Mayevsky and Chance, 1982).

In order to assess the functional state of the brain *in vivo*, it is necessary to monitor all or most of the parameters relevant to various brain functions. During the past 30 years, monitoring devices have been developed for that purpose.

One of the most popular devices for monitoring blood flow is the Laser Doppler Flowmeter (LDF). The LDF uses a low power laser (usually helium: neon, 2–3 mW) to generate a low risk (noninjurious) beam of red or infrared light, which passes through an optical fiber to illuminate a region of tissue where the blood flow is measured.

The principle behind LDF is that the emitted laser light (photons) penetrates tissue to a depth, which is dependent on the light frequency. The light is reflected after it strikes either immobile tissue or moving red blood cells; the portion of this light reflected from moving blood cells undergoes a Doppler frequency shift (Wadhvani et al., 1990). By sampling all reflected light via other optical fibers connected to a photodetector, a continuous reading proportional to the local blood flow is obtained. The device can calculate the flux of erythrocytes within the sample volume (Haberl et al., 1989; Bolognese et al., 1993; Haberl et al., 1993). Flux is calculated by multiplying the percentage of light reflected from moving red blood cells by the mean velocity of movement. Most commercially available devices

present the values of tissue blood flow not in absolute units, but rather as relative units using electronic calibration when the probe is inserted in a calibration solution provided by the manufacturer (Perimed, Sweden).

Another significant parameter to be monitored is the NADH redox state. Mayevsky and collaborators (Mayevsky and Chance, 1974; Friedli et al., 1982; Mayevsky, 1983b; Mayevsky and Weiss, 1991; Mayevsky et al., 1998) measured *in vivo* the oxidation–reduction state of intramitochondrial pyridine nucleotides by a multichannel fluorometer-reflectometer. This approach permitted (Kraut et al., 2003) to measure the changes in the mitochondrial redox status (O_2 balance) in four different organs simultaneously (brain, liver, kidney, and testis) in the same animal.

Monitoring of brain energy metabolism, using fiber optic surface fluorometry/reflectometry, has been described in many publications (Mayevsky, 1984, 1993; Mayevsky et al., 1998; Meilin et al., 1999).

The principle of NADH monitoring from the brain surface is as follows. Excitation light (366 nm) passes from the fluorometer to the brain via a bundle of optical fibers made of quartz. The light emitted by NADH (450 nm), along with the reflected light at the excitation wavelength, is transferred to the fluorometer via another bundle of fibers. The changes in the reflected light correlate with the changes in tissue blood volume and also serve to correct for hemodynamic artifacts appearing in NADH measurements (for details see (Mayevsky, 1984). The changes in fluorescence and reflectance signals are calculated relatively to the calibrated signals under normoxic conditions. This type of calibration is not absolutely exact, yet it has provided reliable and reproducible results in different animals and at different laboratories.

The combination of NADH fluorescence and LDF techniques permitted the measurement of a familiar biochemical and physiological process: an increase in NADH levels due to pathological conditions, such as anoxia, hypoxia, and ischemia. On the other hand, conditions that activate brain metabolism, such as spreading depression and/or convulsions, decreased the level of NADH in brain tissue, i.e., NADH was oxidized to NAD (Mayevsky and Chance, 1975; Mayevsky, 1983a; Mayevsky and Sclarsky, 1983). The same results were obtained in ischemic and hypoxic dog's heart (Sonn et al., 1982) and rat's liver (Barbiro et al., 1998).

Once the balance of energy production, supply, and demand is impaired, a cascade of events occurs that finally leads to tissue degeneration (Mayevsky, 1984). Further understanding of the interrelation between the determinants of tissue energy metabolism will enable us to surveil the deterioration/recovery of the tissue under various clinical conditions of oxidative stress. Mathematical modeling makes it possible to monitor only one or two critical variables and compute the others in real time during clinical or experimental procedures. This may allow clinicians to overcome the difficulties and hazards involved in recording all these variables *in vivo*.

3. The model

As mentioned above, in the framework of our research, we refer to the tissue as a whole, i.e., as a self-contained system with inputs and outputs. This

simplification enables us to utilize the so-called integral- or point-model approach, when the physiological variables are regarded as functions of time only (their interdependence apart), rather than as space-distributed variables. Hence, the “diffusion” terms and the spatial derivatives that appear in the space-distributed models (Revett et al., 1998; Ruppin et al., 1999) are omitted, and we arrive at a classical dynamic system, whose states are described by ordinary differential equations of the kinetic type. Furthermore, using this approach, we can tune the model, maximizing the fit to the actual clinical and experimental data with little risk of overfitting. In the course of data fitting, different kinds of nonlinearities in the right-hand parts of the differential equations were tested. The main objective was to keep the model physiologically meaningful, simple as possible, and universal in the sense that the same values of the model parameters would be used to simulate the normal and different pathological conditions of the brain tissue. The goodness-of-fit was examined and confirmed in numerous independent runs using various laboratory and clinical data published earlier (Mayevsky et al., 1984, 1996, 1998; Mayevsky, 1990; Meilin et al., 1999). The mathematical model manifests many of the essential characteristics of the experimental data with regard to certain observable variables, providing a quantitative fit, which is indicative of the model’s reliability. We have tested the ability of the model to correctly reproduce the dynamics of a reduced number of the physiological variables when the dynamics of the remaining variables are inputted in the model. This property of our model may be used in clinical practice—to complement real-time measurements.

Our model is based on the assumption that the tissue functional state is fully determined by the following metabolic variables:

- Concentration of extracellular potassium (K).
- Rate of potassium reuptake (R).
- Blood flow (F).
- Oxygen (O).
- NADH (N).
- Partial impairment (P).

Such a formulation of the model was selected because quantitative data on the rates of change of the model variables are scarce. In clinical conditions, only some of the above tissue parameters, such as the blood flow, the concentration of extracellular potassium, and the level of NADH, can be measured. Other, hidden variables (the rate of potassium reuptake, partial impairment, and the level of oxygen) are either nonmeasurable or not measured at the present. Their meaning of the model variables is detailed below.

The model is constructed as a set of nonlinear differential equations (see below (1)–(6)) that govern the temporal evolution of the above metabolic variables. Each of the main tissue variables, being a function of time, depends also on other physiological variables. Its dynamics are governed by an equation that describes the variable’s behavior under both normoxic and pathological conditions. All variables of the model (including time) are nondimensional, i.e., they are normalized through some scales. To enable computations, these variables are discretized. Thus, each of the above six variables ranges from 0 to 1 while time runs from 0 to 500 units (with some small step).

In the equations, the variables are denoted by a single capital letter (e.g., K , R), while their specific levels—by the same letter with a subscript (e.g., K_{rest}); multiplicative constant factors are denoted by a capital “ C ” and subscripted by a number of indices—capital letters usually designating the related variables. The first index identifies the variable whose dynamic equation contains this constant, while the remaining indices (those appearing after the comma) identify the variables that the constant C modulates. The subscripts ‘rest’ and ‘max,’ respectively, designate the resting value and the absolute ceiling of a variable. The resting value $F_{\text{rest}}=F_{\text{max}}/2$ is equal to the normal level of the blood flow. The initial values of the variables in the model reflect normoxic tissue state.

The equations governing the temporal behavior of the metabolic parameters indicated above are constructed on the following grounds.

The rate of change of the extracellular potassium concentration, K , is modeled as a reaction-diffusion process, which is governed by four terms:

$$\frac{dK}{dt} = C_{K,K}(K - K_{\text{rest}})(K - K_{\vartheta})(K - K_{\text{max}}) + (\delta + P)(K_{\text{max}} - K) - C_{K,R}KR + K_{\text{inj}}. \quad (1)$$

The first, ‘reaction’ term in Eq. (1) models the regenerative processes that generate the sharp rise of extracellular potassium concentration occurring when K crosses the thresholds level K_{ϑ} . The second term represents the diffusion of intracellular potassium in undamaged tissue and intracellular potassium release to the extracellular space resulting from various tissue stresses; here constant δ represents the rate of permanent intracellular potassium leakage in normal tissue; for the meaning of P see Eq. (6) and the explanation appearing immediately before it. The third term reflects the reuptake of potassium by Na/K ATPase pumps. The last term represents an external injection of potassium.

The rate of potassium reuptake, R , is modeled by the following equation:

$$\frac{dR}{dt} = C_{R,\text{NOKR}}NO(K - K_{\text{rest}})(R_{\text{max}} - R) - C_{R,RK}R(K_{\text{max}} - K). \quad (2)$$

Two terms in Eq. (2) affect the rate of potassium reuptake, reflecting the functioning of Na/K pumps. The first term in the right-hand part of (2) models the increase of reuptake with increasing levels of NADH and oxygen. The second term gradually brings Na/K ATPase activity back to its resting level when K values are restored.

The blood flow F is regulated by the equation

$$\frac{dF}{dt} = C_{F,FO}(F_{\text{max}} - F)(O_{\text{rest}} - O) + C_{F,F} \left(\frac{F_{\text{max}}}{2} - F \right) - C_{F,KF}(K - K_{\text{rest}})(F_{\text{rest}} - F). \quad (3)$$

Here the first term represents the dependence of blood supply on the oxygen status and the current flow level. The second term in (3) self-regulates the blood flow toward its base rate. The third term describes variations in the blood flow caused

by an irregular extracellular potassium rise (that may result, e.g, from an injection of potassium). When constructing the last term, the previous tissue state has been taken into account. For that purpose, the coefficient $C_{FFK} = 0$, if the previous value of the blood flow is less than the resting value F_{rest} , otherwise it is taken to equal 0.5.

The energy status of the tissue is determined by oxygen, O . Its level is determined by a competition between the supply and demand terms. The supply term is proportional to the blood flow and current oxygen level. The demand term is an equivalent consumption rate; it involves the oxygen, potassium reuptake rate, and NADH. The resulting equation is

$$\frac{dO}{dt} = C_{O,FO}F(O_{max} - O) - C_{O,NRO}N(RO)^{0.5}. \quad (4)$$

The rate of NADH change is determined by its level, while the consumption rate depends on the potassium reuptake as well as on oxygen:

$$\frac{dN}{dt} = C_{N,N}(N_{max} - N) - C_{N,NRO}N(RO)^{0.5}. \quad (5)$$

Finally, the level of stresses experienced by the tissue is represented by the partial impairment variable P . Its meaning can be understood from Eq. (1): stresses upset the integrity of tissue cells, which results in increasing diffusion of the intracellular potassium to the extracellular space. In a damaging situation, the stores of oxygen deplete, and O becomes insufficient for the Na/K pump functioning. The concentration of extracellular potassium rises and the partial impairment augments. The corresponding equation is:

$$\frac{dP}{dt} = C_{P,OK}(O_{min} - O)(K - K_{rest}). \quad (6)$$

The model is implemented using “Stella” software (High Performance Systems, Inc, <http://www.hps-inc.com/>). The differential equations are replaced with a set of their finite-difference analogs and are integrated numerically. Using this model, we investigate how various pathophysiological manipulations interrelate and influence the recovery process. Note that the same constants are used for all modeled situations.

4. Simulation of pathological conditions

4.1. Regimes susceptible of modeling

The simulation of the different pathophysiological tissue conditions was carried out in the following way:

A variety of ischemic events can be produced if, in Eq. (3), we set $F_{max} < 1$ within a time interval $t_1 < t < t_2$. To mimic the initiation of spreading depression, potassium infusion is simulated, i.e., $K_{inj} > 0$, during a designated time interval.

Table 1 The model coefficients/constants used in simulations.

Parameters	Constant value
F_{rest}	0.5
K_{rest}	0.03
K_{inj}	0.18—during injection, 0—otherwise
N_{rest}	0.4
O_{rest}	0.48
R_{rest}	0.3
P_{rest}	0
K_{ϑ}	0.2
$C_{K,K}$	-0.24
$C_{K,R}$	0.08
$C_{F,KF}$	0—if $F < F_{rest}$, 0.5—otherwise
$C_{F,FO}$	0.75
$C_{F,F}$	0.6
$C_{R,NOKR}$	1.4
$C_{R,K}$	0.048
$C_{O,FO}$	0.1
$C_{O,NRO}$	0.18
$C_{N,N}$	0.5
$C_{N,NRO}$	2
$C_{P,OK}$	0.15
δ	0.01

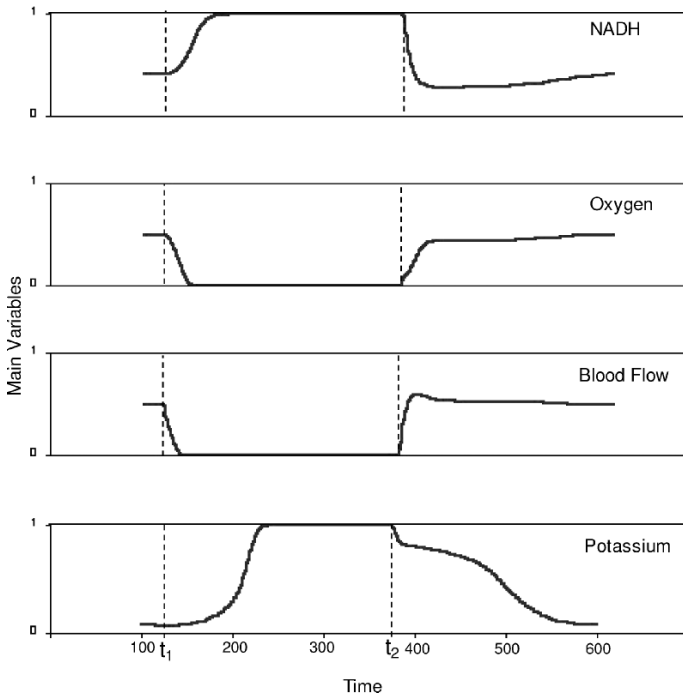


Fig. 1 Simulated Global Ischemia, induced by an abrupt decrease of blood flow to zero level at time t_1 and kept at the zero level until t_2 . The abscissa is nondimensional time, the ordinate—nondimensional main variables (Potassium— K , Blood Flow— F , Oxygen— O , NADH— N).

The initial values of the model variables in all pathological states are their resting levels. The constants and resting values of the parameters are presented in Table 1.

Using our model with the same values of the model coefficients (see Table 1), we have successfully simulated the following pathological states (the results are described further on):

- Global Ischemia;
- Partial Ischemia with depolarization;
- Partial Ischemia without depolarization;
- Spreading Depression;
- Spreading Depression after Partial Ischemia.

We note that 100 time units presented in Figs. 1–5 are approximately equivalent to 1 min. Therefore, for example, the duration of the ischemic condition shown in Fig. 1, is approximately 2.5 min.

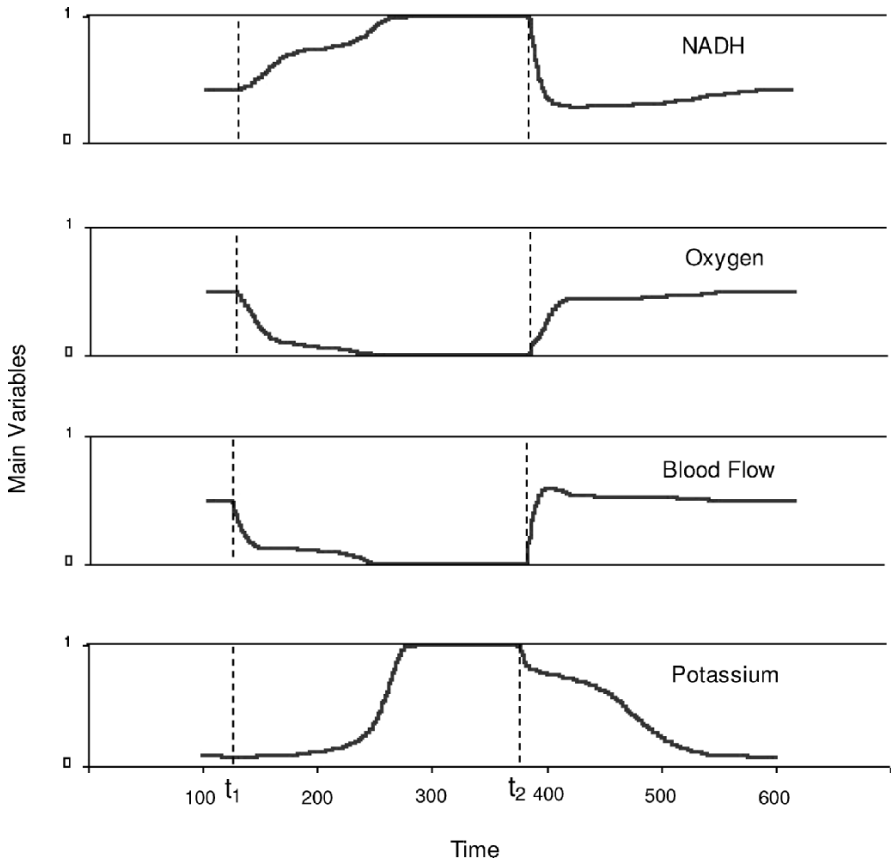


Fig. 2 Simulated Partial Ischemia with depolarization, induced by decreasing the blood flow to a nonzero level during the entire ischemic period (details are as in Fig. 1).

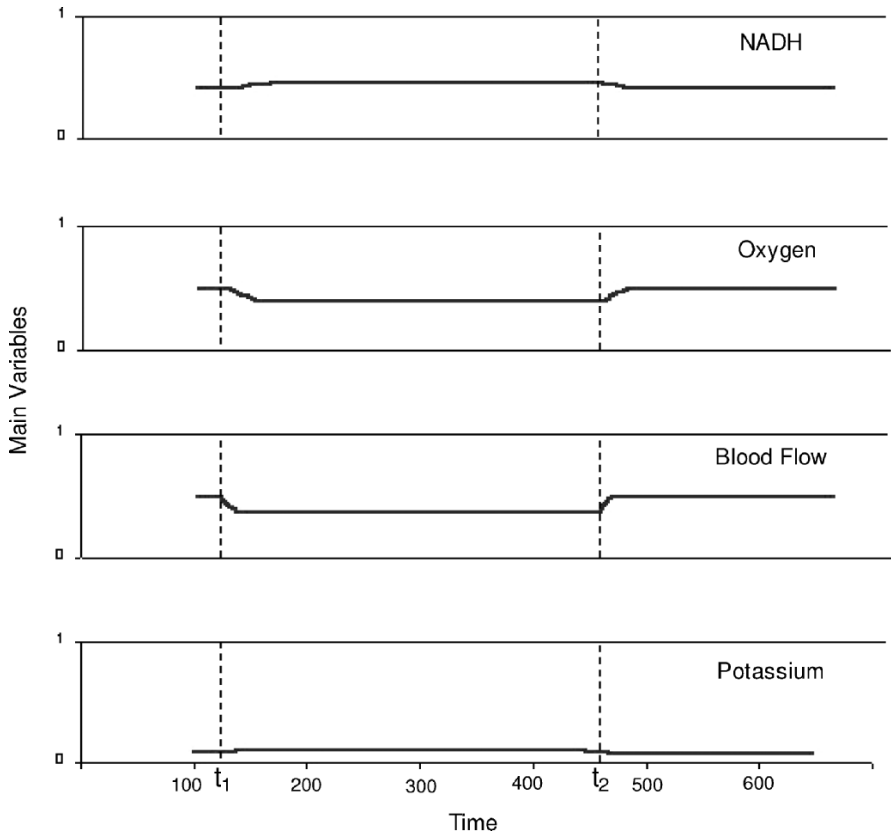


Fig. 3 Simulated Partial Ischemia without depolarization, induced by a mild decrease of blood flow during the entire ischemic period (details are as in Fig. 1).

4.1.1. Global ischemia

Global Ischemia occurs if the blood flow drops to zero. To simulate this condition, F_{\max} is set equal to zero in Eq. (3), within the time interval from t_1 to t_2 (Fig. 1), which signifies that the energy supply terminated, and the Na^+/K^+ pump ceased to operate. This causes an increase in NADH and extracellular potassium to their maxima. In the recovery process, when $t > t_2$, the blood flow increases and reaches a level higher than its resting level (the overshoot or hyperemic response).

4.1.2. Partial ischemia with depolarization

Decreasing the blood flow to a nonzero level simulates this event. In Eq. (3), we fix $F_{\max} = 0.25$ during the ischemic period from t_1 to t_2 . As evident from the data presented in Fig. 2, with the decrease of blood flow, the level of extracellular potassium increases. Only when the potassium level exceeds the threshold value K_g , vasoconstriction occurs, and the blood flow drops to zero. The recovery process is the same as in Global Ischemia.

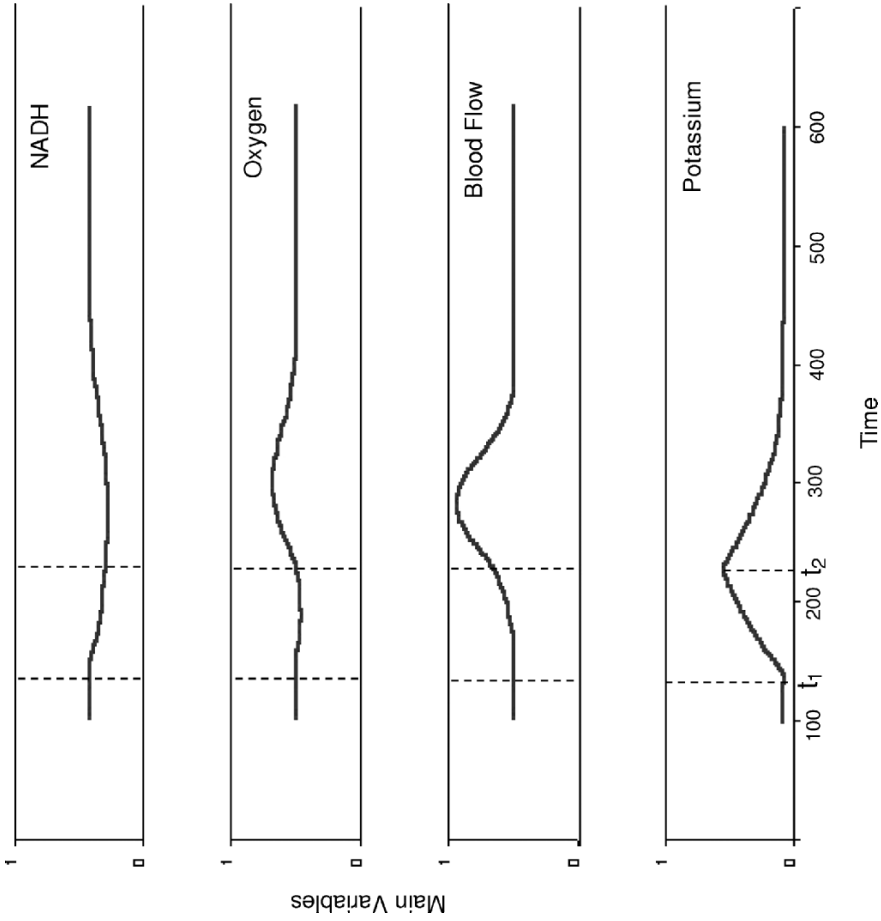


Fig. 4 Simulated Spreading Depression, induced by an injection of potassium when it is at the resting level. The duration of injection is from t_1 to t_2 .

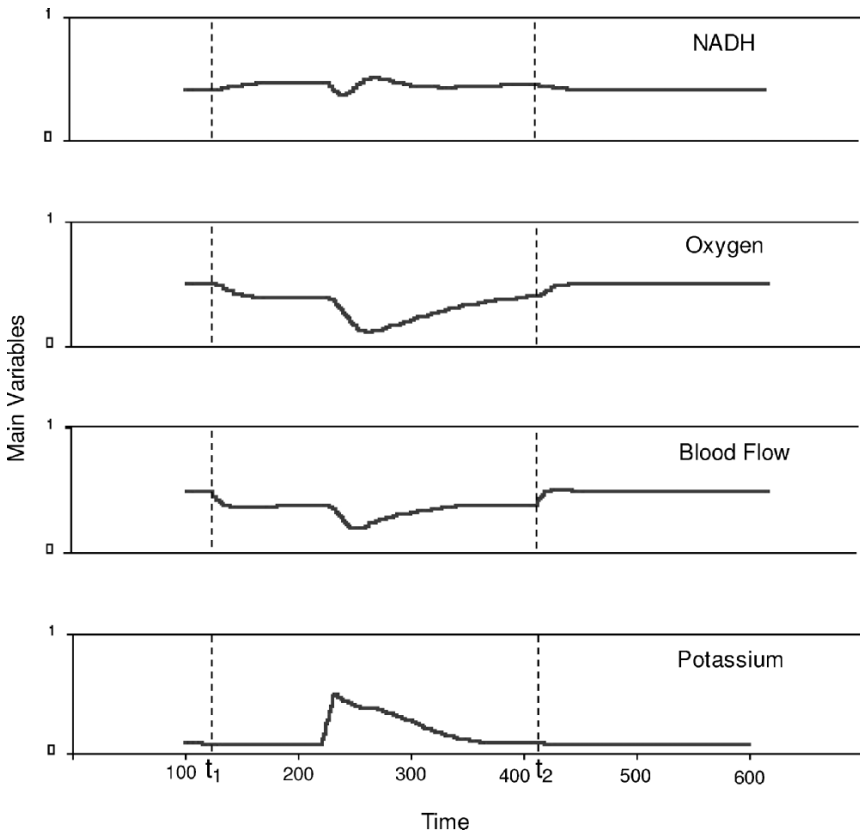


Fig. 5 Simulated Spreading Depression induced after Partial Ischemia, resulting from a mild decrease in blood flow with a short injection of potassium.

4.1.3. Partial ischemia without depolarization

The main principles of simulation remain the same as in Global Ischemia. However, to simulate a more mild decrease of blood flow occurring in the penumbral tissue regions we set $F_{\max} = 0.5$ in Eq. (3) for a certain time interval. The recovery process is the same as in Global Ischemia (Fig. 3).

4.1.4. Spreading depression

The pathological state of spreading depression can be induced by washing the cerebral cortex with a diluted solution of KCl (the “potassium injection”). This is modeled by putting $K_{\text{inj}} > 0$ within the time interval $t_1 < t < t_2$. When spreading depression is induced, the increase in energy requirement leads to the activation of $\text{Na}^+\text{-K}^+$ ATPase in order to restore the normal potassium distribution, and causes an increase in blood flow and a decrease in NADH (Fig. 4).

4.1.5. Spreading depression after partial ischemia

In this case, the blood flow decreases mildly ($F_{\max} = 0.5$ within the time interval from t_1 to t_2), but within the ischemic period, an infusion of potassium is modeled;

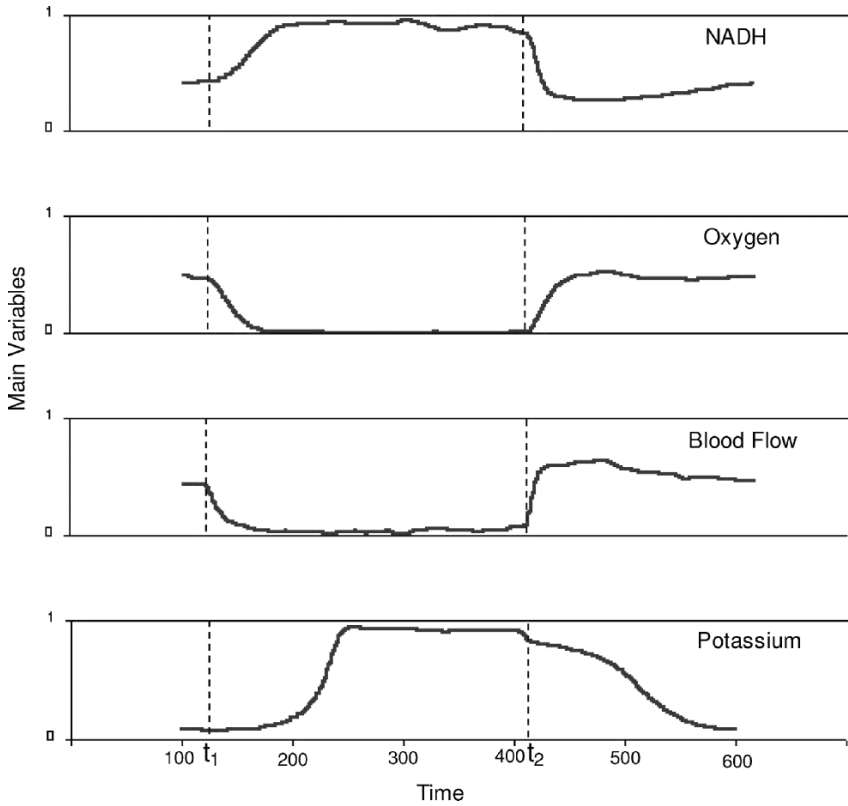


Fig. 6 Global Ischemia simulated by using experimental data on blood flow alteration instead of the blood flow equation (for details see text).

i.e., K_{inj} is assumed to be positive within a relatively short time interval contained in the interval $t_1 < t < t_2$ during which the main events occur. Accordingly, the blood flow slightly decreases as a result of the infusion, and then increases to the new resting level (Fig. 5).

4.2. Simulated versus experimental dynamics

To test the ability of our model to reveal the ‘hidden’ dynamics based on the measured ones, we excluded Eq. (3) from the set of model equations and, instead, used in Eq. (4) the experimental blood flow; the remaining variables were computed according to the corresponding equations. The results of this test are shown in Fig. 6. The temporal behaviors of NADH, oxygen, and potassium were compared with the actual data and were found satisfactory. Simulations of this kind enable us (i) to calibrate the model qualitatively, and (ii) to perform computation of the variables that cannot be measured in clinical conditions so as to predict their behavior during tissue damage and in the recovery period.

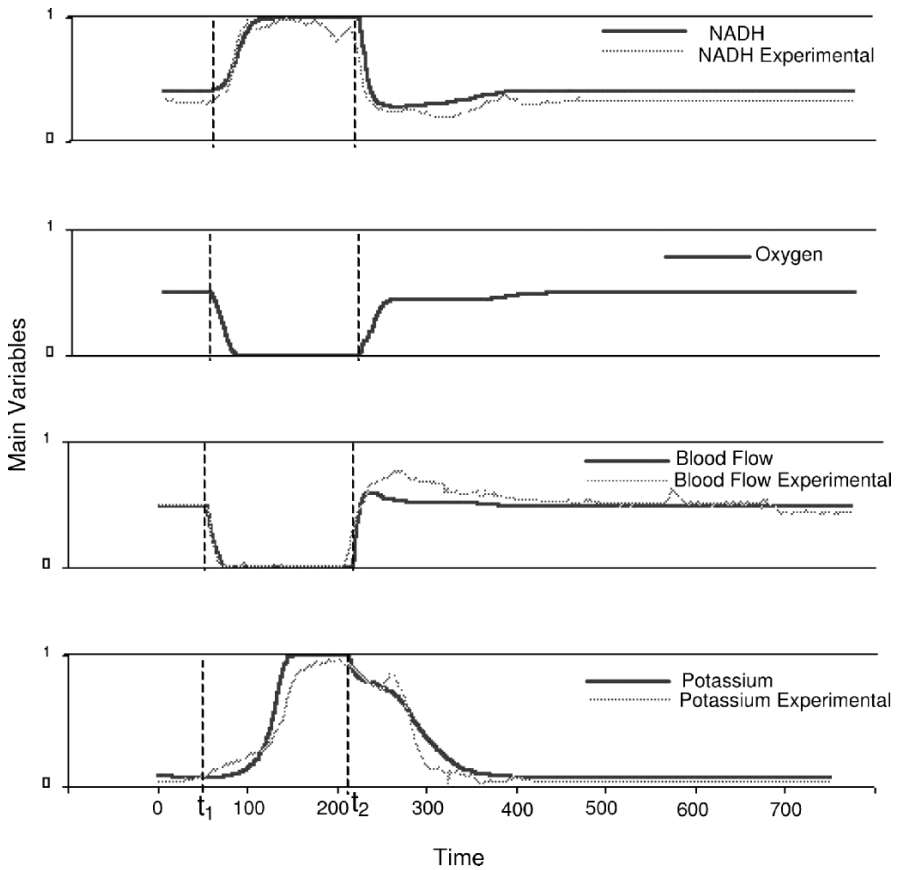


Fig. 7 The comparison of the temporal behavior of the model variables to the corresponding experimental data for Global Ischemia. The simulated dynamics (shown in Fig. 1) overlap with the experimental data from (Mayevsky, 1992).

In the cases of Global Ischemia and Spreading Depression, the temporal behavior of the model variables was compared with the corresponding published clinical and experimental data (Mayevsky et al., 1998; Meilin et al., 1999). In order to compare the simulated and experimental dynamics, the scales were adjusted. The comparison (Figs. 7 and 8) testifies to the qualitative agreement between the computed and experimental values.

5. Discussion

Our results demonstrate the potential of the computational mathematical model of tissue metabolism to describe the pathogenesis of tissue sustains in various clinical and experimental situations. The model simulates five pathophysiological tissue conditions, shown in Figs. 1–5. Note that the various states of tissue activity are

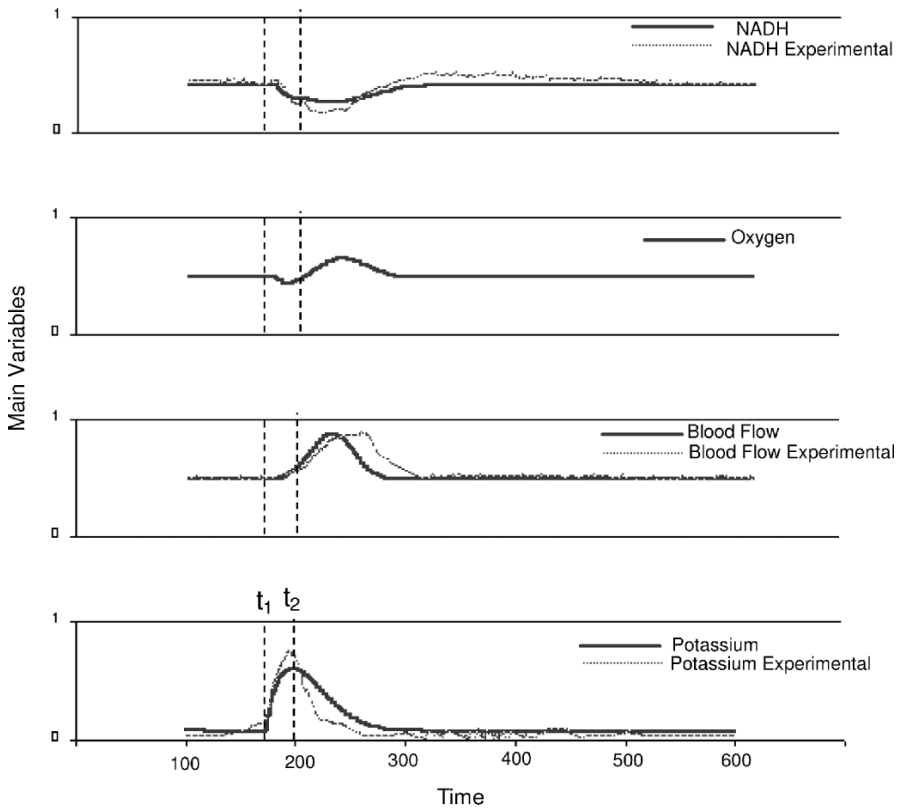


Fig. 8 The comparison of the temporal behavior of the model variables to the corresponding clinical data for Spreading Depression from Mayevsky et al. (1996).

described using the same values of constants (Table 1). This indicates the model's adequacy for the processes occurring in the tissue. The considerable qualitative and quantitative agreement with the experimental/clinical data (Figs. 7 and 8) attests to the model's reliability. The number of variables routinely monitored in clinical situations is limited. Using our model in clinical and laboratory practice, the number of measured parameters can be minimized, since the nonmeasured variables can be evaluated by the model in real time. Moreover, in principle, the comparison of the computed and clinical data can be used to test the tissue state and predict the recovery process. When utilized along with real-time clinical measurements, the model may provide the physician with a means for early diagnosis of pathological processes at their early stages.

A wide range of pathological events may ensue due to the limitation of oxygen supply to the tissue by a restriction of blood flow (ischemia) or by a lowering of O_2 level in the inspired air (hypoxia). As a result of oxygen restriction, the mitochondrial activity is inhibited, the ATP production decreases, and the ionic homeostasis is disturbed, leading to extracellular K^+ accumulation. A high correlation has been found between changes in the cerebral blood flow and mitochondrial

NADH redox state during ischemia (Mayevsky, 1990). On the other hand, high levels of extracellular potassium produced in spreading depression (SD) lead to an increase in the tissue metabolic demands, as indicated by a rise in O_2 consumption (Mayevsky and Weiss, 1991). This process is usually accompanied by an increase in blood flow; as a result, the activation of mitochondrial activity leads to NADH oxidation.

In our recent publications (Mayevsky et al., 2002, 2004; Pevzner et al., 2003), we have described the principles behind a new medical device, the TiSpec-Tissue Spectroscope. The TiSpec provides real-time data on three optical variables, namely, the tissue blood flow, mitochondrial NADH redox state, and tissue reflectance. It is expected that by using this device in various clinical situations, the three parameters provided will permit diagnosing the tissue metabolic state, even though extracellular K^+ and O_2 levels are not monitored. Joining these measurements with the data processing by our model will open up the possibility of expanding the scope of experiments where the control parameters F_{\max} , K_{inj} , and the time of injection would alter within given realistic intervals. The aim of such experiments will be the evaluation of the optimal values (or frames) of the variables that determine the required behaviors of NADH and oxygen.

References

- Bailey, J.E., 1998. Mathematical modeling and analysis in biochemical engineering: Past accomplishments and future opportunities. *Biotechnol. Prog.* 14, 8–20.
- Barbiro, E., Zurovsky, Y., Mayevsky, A., 1998. Real time monitoring of rat liver energy state during ischemia. *Microvasc. Res.* 56, 253–260.
- Bolognese, P., Miller, J.J., Heger, I.M., Milhorat, T.H., 1993. Laser-Doppler flowmetry in neurosurgery. *J. Neurosurg. Anesthesiol.* 5, 151–158.
- Chance, B., Oshino, N., Sugano, T., Mayevsky, A., 1973. Basic principles of tissue oxygen determination from mitochondrial signals. In: *Advances in Experimental Medicine and Biology*. Plenum, New York, pp. 239–244.
- Erecinska, M., Silver, I.A., 1989. ATP and brain function. *J. CBF Metab.* 9, 2–19.
- Friedli, C.M., Sclarsky, D.S., Mayevsky, A., 1982. Multiprobe monitoring of ionic, metabolic and electrical activities in the awake brain. *Am. J. Physiol.* 243, R462–R469.
- Gershenfeld, N.A., 1999. *The Nature of Mathematical Modeling*. Cambridge: Cambridge University Press.
- Gombert, A., Nielsen, J., 2000. Mathematical modelling of metabolism. *Curr. Opin Biotechnol.* 11, 180–186.
- Haberl, R.L., Heizer, M.L., Marmarou, A., Ellis, E.F., 1989. Laser Doppler assessment of brain microcirculation: Effect of systemic alterations. *Am. J. Physiol.* 256, H1247–H1254.
- Haberl, R.L., Villringer, A., Dirnagl, U., 1993. Applicability of laser-Doppler flowmetry for cerebral blood flow monitoring in neurological intensive care. *Acta Neurochir. Suppl. (Wien)* 59, 64–68.
- Hatzimanikatis, V., Floudas, C., Bailey, J., 1995. A mathematical model for the G1/S transition of the mammalian cell cycle. *Biotechnol. Lett.* 17, 669–674.
- Hudetz, A. G., 1999. Mathematical model of oxygen transport in the cerebral cortex. *Brain Res.* 817, 75–83.
- Kraut, A., Barbiro-Michaely, E., Zurovsky, Y., Mayevsky, A., 2003. Multiorgan monitoring of hemodynamic and mitochondrial responses to anoxia and cardiac arrest in the rat. *Adv. Exp. Med. Biol.* 510, 299–304.
- Mayevsky, A., Manor, T., Pevzner, E., Deutsch, A., Etziony, R., Dekel, N., Jaronkin, A., 2004. Tissue spectroscope: a new *in vivo* approach to monitor tissue vitality in real time. *J. Biomed. Optics.* 9, 1028–1045.

- Mayevsky, A., 1983a. Metabolic, ionic and electrical responses to experimental epilepsy in the awake rat. In: Baldy, M., Moulinier, D.H., Ingvar, D.H., Meldrum, B.S. (Eds.), *Proceedings of the First International Congress of Cerebral Blood Flow, Metabolism and Epilepsy*. John Libbey, pp. 263–270, London, England.
- Mayevsky, A., 1983b. Multiparameter monitoring of the awake brain under hyperbaric oxygenation. *J. Appl. Physiol.* 54, 740–748.
- Mayevsky, A., 1984. Brain NADH redox state monitored in vivo by fiber optic surface fluorometry. *Brain Res. Rev.* 7, 49–68.
- Mayevsky, A., 1990. Level of ischemia and brain functions in the Mongolian gerbil in vivo. *Brain Res.* 524, 1–9.
- Mayevsky, A., 1992. Cerebral blood flow and brain mitochondrial redox state responses to various perturbations in gerbils. *Adv. Exp. Med. Biol.* 317, 707–716.
- Mayevsky, A., 1993. Biochemical and physiological activities of the brain as in vivo markers of brain pathology. In: Bernstein, E.F., Callow, A.D., Nicolaidis, A.N., Shifrin, E.G. (Eds.), *Cerebral, Revascularization*. Med-Orion, pp. 51–69, London, England.
- Mayevsky, A., Chance, B., 1974. Repetitive patterns of metabolic changes during cortical spreading depression of the awake rat. *Brain Res.* 65, 529–533.
- Mayevsky, A., Chance, B., 1975. Metabolic responses of the awake cerebral cortex to anoxia, hypoxia, spreading depression and epileptiform activity. *Brain Res.* 98, 149–165.
- Mayevsky, A., Chance, B., 1982. Intracellular oxidation reduction state measured in situ by a multichannel fiber-optic-surface fluorometer. *Science* 217, 537–540.
- Mayevsky, A., Doron, A., Manor, T., Meilin, S., Zarchin, N., Ouaknine, G.E., 1996. Cortical spreading depression recorded from the human brain using a multiparametric monitoring system. *Brain Res.* 740, 268–274.
- Mayevsky, A., Manor, T., Pevzner, E., Deutsch, A., Etziony, R., Dekel, N., 2002. Real-time optical monitoring of tissue vitality in vivo. *SPIE* 4616, 30–39.
- Mayevsky, A., Meilin, S., Manor, T., Ornstein, E., Zarchin, N., Sonn, J., 1998. Multiparametric monitoring of brain oxygen balance under experimental and clinical conditions. *Neurol. Res.* 20, S76–S80.
- Mayevsky, A., Sclarsky, D.S., 1983. Correlation of brain NADH redox state, K^+ , PO_2 and electrical activity during hypoxia, ischemia and spreading depression. In: *Oxygen Transport to Tissue*, vol. IV. Plenum, New York, pp. 129–141.
- Mayevsky, A., Weiss, H.R., 1991. Cerebral blood flow and oxygen consumption in cortical spreading depression. *J. CBF Metab.* 11, 829–836.
- Mayevsky, A., Zarchin, N., Tannenbaum, B., 1984. Brain responses to experimental oxygen deficiency in the Mongolian gerbil. In: Bruley, D., Bicher, H.I., Reneau, D. (Eds.), *Oxygen Transport to Tissue*, vol. VI. Plenum, New York, pp. 191–202.
- Meilin, S., Zarchin, N., Mayevsky, A., 1999. Inter-relation between hemodynamic, metabolic, ionic and electrical activities during ischemia and reperfusion in the gerbil brain. *Neurol. Res.* 21, 699–704.
- Pevzner, E., Deutsch, A., Manor, T., Dekel, N., Etziony, R., Derzy, I., Razon, N., Mayevsky, A., 2003. Real-time multiparametric spectroscopy as a practical tool for evaluation of tissue vitality in vivo. In: Vo-Dinh, T., Grundfest, W.S., Benaron, D.A., Cohn, G.G. (Eds.), *Advances Biomedical and Clinical Diagnostic Systems, Proceedings of the SPIE*, pp. 171–182. SPIE-The International Society for Optical Engineering, Washington D.C., USA.
- Reggia, J.A., Ruppin, E., Berndt, R.S., 1997. Computer modeling: A new approach to the investigation of disease. *MD Comput.* 14, 160–164.
- Revett, K., Ruppin, E., Goodall, S., Reggia, J.A., 1998. Spreading depression in focal ischemia: A computational study. *J. CBF Metab.* 18, 998–1007.
- Ruppin, E., Ofer, E., Reggia, J.A., Revett, K., Goodall, S., 1999. Pathogenic mechanisms in ischemic damage: A computational study. *Comput. Biol. Med.* 29, 39–59.
- Sonn, J., Mayevsky, A., Acad, B., Guggenheimer, E., Kedem, J., 1982. Effect of local ischemia on the myocardial oxygen balance and its response to heart rate elevation. *Q. J. Exp. Physiol.* 67, 335–348.
- Wadhvani, K.C., Rapoport, S.I., 1990. Blood flow in the central and peripheral nervous systems. In: Shepherd, A.P., Oberg, P.A. (Eds.), *Laser Doppler Blood Flowmetry*. Kluwer Academic, Boston, pp. 265–304.